


**Discrete-time quantum walk with time-correlated noise**Y. F. Peng <sup>1</sup>, W. Wang,<sup>1,\*</sup> and X. X. Yi<sup>1,2</sup><sup>1</sup>*Center for Quantum Sciences and School of Physics, Northeast Normal University, Changchun 130024, China*<sup>2</sup>*Center for Advanced Optoelectronic Functional Materials Research and Key Laboratory for UV Light-Emitting Materials and Technology of Ministry of Education, Northeast Normal University, Changchun 130024, China*

(Received 24 November 2020; revised 7 February 2021; accepted 12 February 2021; published 3 March 2021)

The dynamics of a discrete-time quantum walk subject to time-correlated noise is studied in this paper. The noise, which goes beyond the usual telegraph noise with random variables 1 and  $-1$ , is modeled as a unitary coin-type operator and it is generated by a sample path of the Ornstein-Uhlenbeck process. Up to the first order in the amplitude of noise, a master equation to describe the walk is derived. The dynamics governed by the master equation is in good agreement with those given by numerical simulations within a certain number of steps, depending on the parameters of noise. Two remarkable features of long-time dynamics are observed in the numerical simulations. (1) In the slow noise regime, with the increase of the noise amplitude, the quantum coherence is suppressed, and the dynamics of noisy discrete-time quantum walk gradually transits to that of classical random walk. (2) In the fast noise regime, the walker is confined into a few lattice sites, and the width of the wave packet is much narrower compared with that in the slow noise regime.

DOI: [10.1103/PhysRevA.103.032205](https://doi.org/10.1103/PhysRevA.103.032205)**I. INTRODUCTION**

The quantum walk (QW), a natural and straightforward generalization of the classical random walk (CRW) to the quantum world, is currently a topic of great interest to both theorists and experimentalists [1–3]. Compared with CRW, where information propagates at a speed  $\sqrt{t}$ , one of those crucial features that QW possesses is a much faster expansion of walker proportional to  $t$  in position space due to quantum coherence. At certain computational tasks, the QW provides exponential speedup over classical computation and is used as a powerful tool in the most efficient quantum algorithms [2,4,5]. Moreover, with the ability to engineer and control the dynamics of QW by controlling various parameters in evolution operators, the QW can also be used to model a wide variety of physical process including photosynthesis [6–8], quantum diffusion [9], optical or spin pumping and vortex transport [10,11], electrical breakdown [12], localization [13,14], topological phase [15–20], and so on. Motivated by the prospect of such an array of applications, QW are implemented in numerous experimental setups including quantum optical lattices [21,22], ion traps [23–25], photons [18,26–31], and nuclear magnetic resonance [32,33]. These systems offer the possibility to study the quantum dynamics of single or many particles in a precisely controlled experimental setting.

Categorized into two types, the dynamics of the walker is determined completely by a unitary time evolution. In the continuous-time quantum walk (CTQW) [34], the dynamics is described by a Hamiltonian, which defines an evolution continuous in time but discrete in space, without coinlike degrees

of freedom. In the discrete-time quantum walk (DTQW) [35], its dynamics is generally implemented by combining conditional shift operators and coin operators, which act on the position of a walker and its associated coin, respectively, and the system evolves in position space taking the interference of amplitudes of multiple traversing paths [36–39] into account.

In practice, a realistic application of QW should take disorder induced by noise and imperfections into account. The lattice dynamics of the disordered continuous-time quantum walk has been studied for many years, and a key feature (i.e., the localization effect) was found in studies of the role played by system dimensionality [40], correlations [41], and electron-electron interaction [42]. Different variations of the standard DTQW have also been proposed, such as two entangled particles [43], entangled coins [44], multistates [45,46], and different quantum coins in a certain sequence [47]. For a dynamic disorder, the quantum coins are identical for all lattice sites, but they change for every step or several steps [48–50]. The analysis of the time evolution of a quantum walker in the presence of unitary noise in the Hadamard walk showed that the standard deviation of the spatial distribution acquires a diffusive behavior for long steps, similar to the CRW.

Considering these studies of noisy DTQW are mainly focused on the influence of time-uncorrelated or space-correlated noise on dynamics, one may wonder how the dynamics of DTQW changes due to time-correlated noises. Furthermore, since noise is introduced to model the interaction between the system and the environment, the dynamics averaged over noise realizations should be equivalent to a master equation. Then what is the master equation for a DTQW subject to noise?

The remainder of this paper will try to answer these questions as follows: In Sec. II we introduce the model for a

\*wangw100@nenu.edu.cn

DTQW subject to time-correlated noise. In Sec. III we derive a master equation for the noisy DTQW and discuss the influence of noise parameters on the valid time of the master equation. In Sec. IV numerical simulations of noisy dynamics are explored. Section V closes the paper with some concluding remarks.

## II. NOISY SPLIT-STEP QUANTUM WALK

In the CTQW, one can directly define the walk on the position Hilbert space. In the DTQW, in addition to position Hilbert space, it is necessary to introduce a quantum coin operation in a coin Hilbert space to define the direction in which the particle has to move. Due to the coin degree of freedom, the DTQW can be represented by a split-step quantum walk (SSQW), which acts on a single spin-1/2 particle ( $|\uparrow\rangle, |\downarrow\rangle$ ) in a one-dimensional lattice ( $|x\rangle, x \in \mathbb{Z}$ ), reminiscent of the position and coin Hilbert space. Parametrized by angles  $\theta_1$  and  $\theta_2$ , a single SSQW can be defined by the time evolution operator

$$\hat{U}_s = T_\downarrow R_y(\theta_2) T_\uparrow R_y(\theta_1). \quad (1)$$

This protocol consists of a sequence of unitary operations:

$$\begin{aligned} R_y(\theta) &= \sum_x e^{-i\theta\sigma_y/2} \otimes |x\rangle\langle x|, \\ T_\uparrow &= \sum_x |x+1\rangle\langle x| \otimes |\uparrow\rangle\langle\uparrow| + |x\rangle\langle x| \otimes |\downarrow\rangle\langle\downarrow|, \\ T_\downarrow &= \sum_x |x\rangle\langle x| \otimes |\uparrow\rangle\langle\uparrow| + |x-1\rangle\langle x| \otimes |\downarrow\rangle\langle\downarrow|. \end{aligned} \quad (2)$$

The particle in the SSQW, like other quantum system in the practical world, would inevitably interact with the environment. This interaction can be described by a variety of noise models. Here we employ a unitary noise operator given in [48,51,52] that reads

$$\hat{U} = \hat{U}_s \hat{U}_A, \quad (3)$$

where  $\hat{U}_A = \sum_x e^{-i\hat{A}(t)} \otimes |x\rangle\langle x|$ ,  $\hat{U}_s$  is the time evolution operator of the noiseless SSQW, and  $\hat{A}(t)$  is a Hermitian operator determined by the environment. In terms of the Pauli matrix,  $\hat{A}(t)$  can be written as

$$\hat{A}(t) = \lambda_x(t)\sigma_x + \lambda_y(t)\sigma_y + \lambda_z(t)\sigma_z, \quad (4)$$

where  $\lambda_v(t)$ ,  $v = x, y, z$  are real stochastic variables and  $\sigma_{x,y,z}$  are Pauli operators. The dynamics of the walker can be calculated by the ensemble average [53,54]

$$\rho(t) = \langle \hat{U}(t) \rho(0) \hat{U}^\dagger(t) \rangle, \quad (5)$$

where  $\rho(0)$  is the initial density matrix and  $\langle \dots \rangle$  denotes the average of unitary dynamics over all possible realizations of the stochastic processes. Here, for simplicity, we assume that  $\lambda_v(t) = \gamma_v \zeta_v(t)$ .  $\zeta_v(t)$  comes from a Gaussian process satisfying

$$\langle \zeta_v(t) \rangle = 0, \quad \langle \zeta_v(t) \zeta_{v'}(t') \rangle = \delta_{v,v'} K(t, t'). \quad (6)$$

Although DTQW can be implemented by linear optical components as in [29], this increases the experimental complexity in terms of optical stability, alignment, and cost. Based on [26], we present a scheme to implement the noisy SSQW

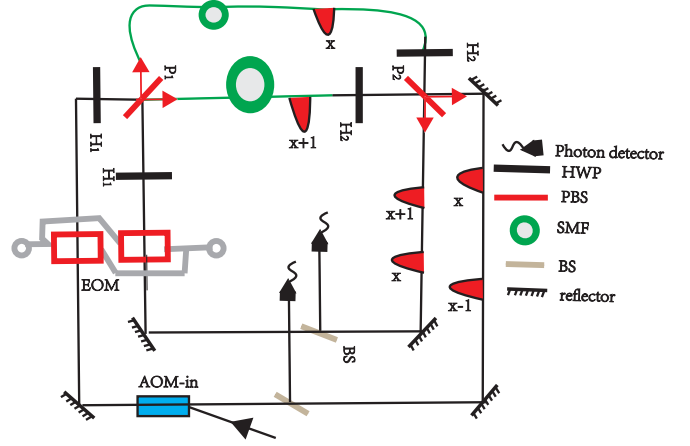


FIG. 1. Sketch of the setup. The initial pulse is from a pulsed laser and coupled into the circuit by an acousto-optic modulator (AOM).  $H_1$  and  $H_2$  represent the rotation operations  $R_y(\theta_1)$  and  $R_y(\theta_2)$ , respectively.  $P_1$  and  $P_2$  are introduced to realize the step operations  $T_1$  and  $T_2$ , respectively. The gray circles of the EOM represent the input and output of external voltage, respectively. Two green circles represent two SMFs with different lengths to produce temporally encoded states.

on an optical feedback loop as illustrated in Fig. 1. In this scheme, different path lengths in the circuit generate temporally encoded states where different position states are represented by discrete-time bins. The stochastic unitary operation  $e^{-i\hat{A}(t)}$  is implemented by two electro-optic modulators (EOMs) that always maintain the same input electric field to output the same stochastic signals. Two coin operations  $R_y(\theta_1)$  and  $R_y(\theta_2)$  are implemented by half-wave plate (HWP)  $H_1$  and  $H_2$ , separately. The photonic wave packets are split by a polarizing beam splitter (PBS)  $P_1$  and routed through single-mode fibers (SMF) of different length, which are labeled by  $x+1$  and  $x$ , respectively. Considering the packet  $x$  arrives at  $P_2$  firstly, therefore, in chronological order the wave packets are  $x-1$ ,  $x$  and  $x, x+1$  are detected successively. Then some photons are reflected by a beam splitter (BS) for detection and the transmitted photons continue to go through the circuit.

## III. MASTER EQUATION OF NOISY SSQW

The effects of noise in coin operator or conditional translation on the behaviors of a DTQW have been extensively studied [48,50,55]. These studies have pointed that the dynamics of noisy DTQW averaged over all possible realizations equals that of a walker interacting with the environment; however, the expression for the master equation is still unknown. Faced with this problem, we derive a master equation in the following. The reduced dynamics of a system embedded in an environment is generally described by a master equation of the following form:

$$\frac{d}{dt} \rho(t) = -\frac{i}{\hbar} [\hat{H}_s, \rho(t)] + \mathcal{D}[\rho(t)], \quad (7)$$

where  $\rho(t)$  is the reduced density matrix of the walker with Hamiltonian  $\hat{H}_s$  coupled to the environment. The first term on the right-hand side accounts for the unitary part of the

evolution, The second term accounts for the nonunitary dynamics resulting from the interaction with the environment. In this picture decoherence is simulated by averaging over an ensemble of these stochastic but unitary quantum dynamics. Although the step protocol is defined explicitly in terms of the discrete unitary operations  $T_{\uparrow,\downarrow}$  and  $R_y(\theta)$ , the resulting evolution over one step is equivalent to that generated by a time-independent effective Hamiltonian over the step time, i.e.,  $e^{-i\hat{H}_s} = \hat{U}_s$ . Based on the translational symmetry of the system under study, in the quasimomentum basis  $|k\rangle = (1/\sqrt{2\pi})\sum_k e^{-ikx}|x\rangle$ , the effective Hamiltonian  $\hat{H}_s$  can be written as

$$\hat{H}_s = \sum_k [E_k \vec{n}_k \cdot \vec{\sigma}] \otimes |k\rangle\langle k|. \quad (8)$$

The energy and the components of the Bloch vector are given by

$$\cos E_k = \cos(\theta_1/2) \cos(\theta_2/2) \cos k - \sin(\theta_1/2) \sin(\theta_2/2), \quad (9)$$

and  $\vec{n}_k = n_x \vec{i} + n_y \vec{j} + n_z \vec{k}$ , with

$$\begin{aligned} n_x &= \frac{\sin(\theta_1/2) \cos(\theta_2/2) \sin k}{\sin E(k)}, \\ n_y &= \frac{\cos(\theta_1/2) \sin(\theta_2/2) + \sin(\theta_1/2) \cos(\theta_2/2) \cos k}{\sin E(k)}, \\ n_z &= \frac{-\cos(\theta_1/2) \cos(\theta_2/2) \sin k}{\sin E(k)}. \end{aligned} \quad (10)$$

$\hat{U} = e^{-i\hat{H}_s} e^{-i\hat{A}(t)} = e^{-i\hat{H}(t)}$ , up to the first-order commutation relation of the Baker-Campbell-Hausdorff (BCH) formula, this approximate expression for  $\hat{H}(t)$  is written as

$$\hat{H}_{st}(t) = \hat{H}_s + \sum_\nu \lambda_\nu(t) \hat{L}_\nu, \quad (11)$$

where  $\nu = x, y, z$  with

$$\begin{aligned} \hat{L}_x &= \sum_k [\sigma_x - E_k (\vec{n} \times \vec{\sigma})_x] \otimes |k\rangle\langle k|, \\ \hat{L}_y &= \sum_k [\sigma_y - E_k (\vec{n} \times \vec{\sigma})_y] \otimes |k\rangle\langle k|, \\ \hat{L}_z &= \sum_k [\sigma_z - E_k (\vec{n} \times \vec{\sigma})_z] \otimes |k\rangle\langle k|. \end{aligned} \quad (12)$$

The Hamiltonian of the quantum simulator,  $\hat{H}_{st}(t)$ , is composed of the target Hamiltonian,  $\hat{H}_s(t)$ , and a stochastic part that includes a set of Hermitian operators  $\hat{L}_\nu$  with noisy coupling  $\lambda_\nu(t)$ . This stochastic part will be used to engineer the dissipator in Eq. (7).

The stochastic density matrix corresponding to one realization of the Gaussian processes,  $\rho_{st}(t) = |\psi_{st}(t)\rangle\langle\psi_{st}(t)|$ , is given in terms of the pure state  $|\psi_{st}(t)\rangle$ , which is obtained from the exact solution of the Schrödinger equation generated by the stochastic Hamiltonian implemented in the simulator  $\hat{H}_{st}(t)$  in Eq. (11),

$$\frac{d}{dt} \rho_{st}(t) = -i[\hat{H}_s, \rho_{st}(t)] - i \sum_\nu \gamma_\nu [\zeta_\nu(t) \hat{L}_\nu, \rho_{st}(t)], \quad (13)$$

where  $\zeta_\nu$  was introduced to describe the stochastic processes. Averaging over different realizations of stochastic processes  $\zeta_\nu(t)$ , we obtain the dynamics for the noise-averaged density

matrix

$$\frac{d}{dt} \langle \rho_{st}(t) \rangle = -i[\hat{H}_s, \langle \rho_{st}(t) \rangle] + \mathcal{D}[\rho_{st}(t)], \quad (14)$$

where  $\mathcal{D}[\rho_{st}(t)] = -i \sum_\nu \gamma_\nu [\hat{L}_\nu, \langle \zeta_\nu(t) \rho_{st}(t) \rangle]$ . Comparing Eq. (14) with Eq. (7), the master equation describing the reduced dynamics of open systems, enables us to identify the second term on the right-hand side as a dissipator responsible for an effective nonunitary evolution of the noise-averaged density matrix. Since the stochastic density matrix is a functional of the stochastic field  $\zeta_\nu(t)$ , the explicit form of the dissipator can be derived by using Novikov's theorem [53,56], which gives the mean value of a product of a Gaussian noise with its functional

$$\langle \zeta_\nu(t) \rho_{st}[\zeta_\nu(t)] \rangle = \int_0^t \langle \zeta_\nu(t) \zeta_\nu(t') \rangle \left\langle \frac{\delta \rho_{st}[\zeta_\nu(t)]}{\delta \zeta_\nu(t')} \right\rangle dt'. \quad (15)$$

The functional derivative can be obtained from the stochastic density matrix  $\rho_{st}(t) = \hat{U}_{st}(t, t') \rho_{st}(t') \hat{U}_{st}^\dagger(t, t')$ , where the time evolution operator  $\hat{U}_{st}(t, t') = \mathcal{T} \exp[-i \int_{t'}^t \hat{H}_{st}(s) ds]$ , and  $\mathcal{T}$  denotes the time-ordering operator. Therefore, partial differentiation reads

$$\frac{\delta \rho_{st}(t)}{\delta \zeta_\nu(t')} = \hat{U}_{st}(t, t') (-i \gamma_\nu [\hat{L}_\nu, \rho_{st}(t')]) \hat{U}_{st}^\dagger(t, t'). \quad (16)$$

Using this expression, the master equation for the noise-averaged density matrix is derived as

$$\begin{aligned} \frac{d}{dt} \langle \rho_{st}(t) \rangle &= -i[\hat{H}_s, \langle \rho_{st}(t) \rangle] - \sum_\nu \gamma_\nu^2 \int_0^t dt' K(t, t') \\ &\quad \times [\hat{L}_\nu, \langle [\hat{U}_{st}(t, t') \hat{L}_\nu \hat{U}_{st}^\dagger(t, t'), \rho_{st}(t')] \rangle]. \end{aligned} \quad (17)$$

In this part the initial state  $|\psi(0)\rangle = |x_0\rangle \otimes (1/\sqrt{2})(|\uparrow\rangle - i|\downarrow\rangle)$  with  $x_0 = 51$  and  $\theta_1 = 0.2\pi$ ,  $\theta_2 = 0.3\pi$ . Here we consider time-correlated Ornstein-Uhlenbeck process

$$\langle \zeta_\nu(t_1) \zeta_{\nu'}(t_2) \rangle = \delta_{\nu\nu'} \gamma^2 e^{-|t_1 - t_2|/\tau}. \quad (18)$$

We are interested in the dynamics with different amplitudes  $\gamma$  and correlation time  $\tau$  of the noise and will discuss the situation that tunes from the Markovian (or white noise limit, i.e.,  $\tau \rightarrow 0$ ) to the limit of the quasistatic noise (i.e.,  $\tau \rightarrow \infty$ ). The selected parameters can well describe the dynamic changes of the system from Markovian to quasistatic noise transition. We compare the distribution of the analytical results obtained from Eq. (17) with those of the numerical results obtained by Eq. (5) and use the similarity  $S$  defined by  $S = [\sum_x \sqrt{P_a(t) P_n(t)}]^2$  [18,26–29] to quantify the equality of two probability distributions ( $S = 0$  for completely orthogonal distributions and  $S = 1$  for identical distributions). As pointed out in the earlier study, although a small imperfection can cause  $\sqrt{S}$  to drop to  $0.807 \pm 0.002$  [30], the two in comparison have no much differences. So, we choose  $S = 0.8$  as the threshold in our case.

*Markovian case.* The form of dissipator greatly simplifies when the stochastic variables  $\{\zeta_\nu(t)\}$  are described by Ornstein-Uhlenbeck with  $\tau = 0.1$ , which can be seen as a white noises and therefore  $K(t, t') = \delta(t - t')$ . In particular, the dissipator now only depends on the average density operator  $\langle \rho_{st}(t) \rangle$  that we hereafter denote by  $\rho(t)$  to simplify the

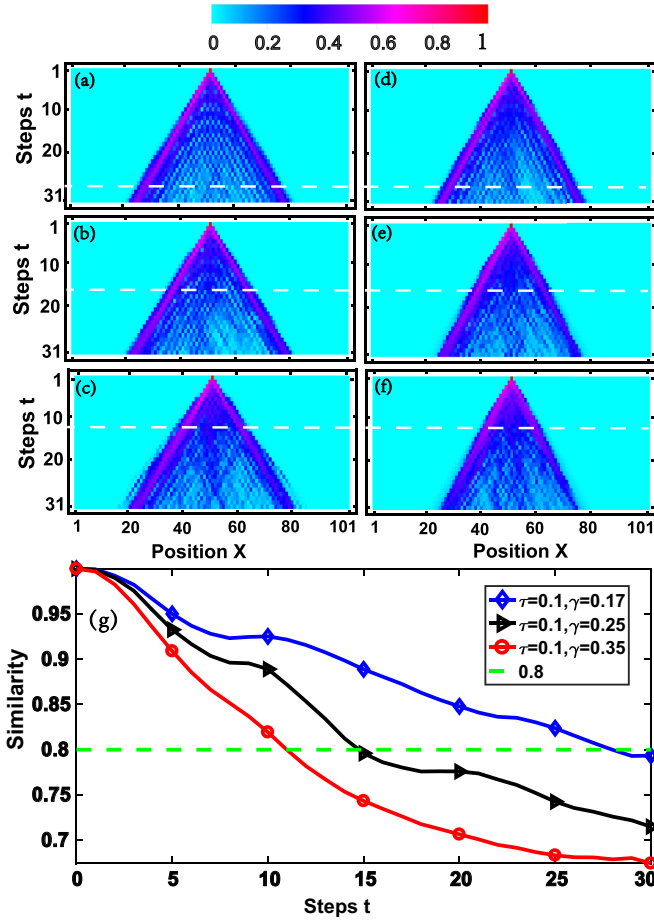


FIG. 2. Time evolution of the density of probability in position space for a quantum walker on chains with  $\gamma_v = \gamma$ . (a)–(c) Analytical space distributions [obtained from Eq. (19)] for  $\tau = 0.1$ ,  $\gamma = 0.17, 0.25, 0.35$ , respectively. (d)–(f) Numerical space distributions [obtained from Eq. (5)] for  $\tau = 0.1$ ,  $\gamma = 0.17, 0.25, 0.35$ , respectively. (g) Similarity as a function of time.

notation. Eq. (17) in this case reduces to

$$\frac{d}{dt}\rho(t) = -i[\hat{H}_s, \rho(t)] - \sum_v \gamma_v^2 [\hat{L}_v, [\hat{L}_v, \rho(t)]]. \quad (19)$$

The dynamics are shown in Fig. 2.

*Generalization to non-Markovian dynamics.* While the use of white noise leads to a Markovian Lindblad dissipator, a non-Markovian evolution can be obtained by the use of colored noise. Up to the second order in the strength of noise, approximating  $\hat{U}_{st}(t, t')$  by  $\hat{U}_s(t, t') \equiv e^{-i\hat{H}_s(t-t')}$ , we can derive a master equation for the walker subject to colored noise

$$\begin{aligned} \frac{d}{dt}\rho(t) = & -i[\hat{H}_s, \rho(t)] \\ & - \sum_v \gamma_v^2 \int_0^t dt' e^{(t-t')/\tau} [\hat{L}_v, [\hat{L}_v(t, t'), \rho(t)]], \end{aligned} \quad (20)$$

where  $\hat{L}_v(t, t') = \hat{U}_s(t, t')\hat{L}_v\hat{U}_s^\dagger(t, t')$ . The probability distributions are shown in Fig. 3.

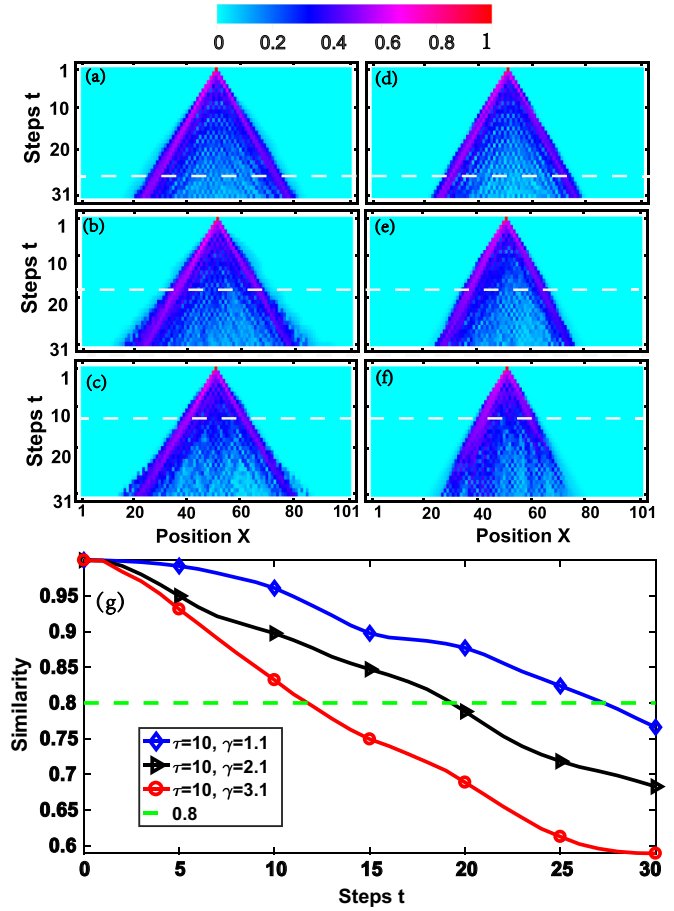


FIG. 3. Time evolution of probability in position space of a quantum walker on chains with  $\gamma_v = \gamma$ . (a)–(c) Analytical results for  $\tau = 10$ ,  $\gamma = 1.1, 2.1, 3.1$  obtained from Eq. (20), and (d)–(f) numerical results for  $\tau = 10$ ,  $\gamma = 1.1, 2.1, 3.1$ , respectively. (g) Similarity as a function of time.

The similarities as functions of time for Markovian and non-Markovian cases are presented in Figs. 2(g) and 3(g), which demonstrate that the similarity decreases with the increase of steps  $t$ . The white-dashed lines in Figs. 2 and 3 are for the similarity between the analytical result and numerical result being greater than 0.8 before reaching the evolution steps  $t$  marked by the white line. If the similarity is greater than 0.8, we would say the master equation derived from Eq. (11) describes well the noisy walk. In fact, noticing the SSQW can be written as  $e^{-i\hat{H}_s}e^{-i\hat{A}(t)}$ , we can rearrange the Hamiltonian and write it as  $e^{-i\hat{H}_s(t)-i\hat{H}_e(t)}$ , so in order to get the Hamiltonian in Eq. (11), we have to ignore  $\hat{H}_e$ . Therefore, with the increase of evolution steps, the impact of the ignored part on the dynamics gradually appears, and the similarity of the two results naturally decreases. The larger the noise amplitude, the greater the influence of this part on dynamics. So the valid time of the master equation is shorter under the same correlation time. This can be easily found from Figs. 2 and 3. Furthermore, Figs. 2(g) and 3(g) show that the steps for the similarity decreasing to the threshold value (i.e., 0.8) for  $\tau = 0.1$ ,  $\gamma = 1.1$  will be much shorter than that for  $\tau = 10$ ,  $\gamma = 1.1$ . Time-correlated noise destroys the time

uniformity of the SSQW and then affects the evolution of the SSQW. Stochastic sequences with longer correlation times  $\tau$  are relatively smoother under the same noise amplitude  $\gamma$  (see Fig. 8 in Appendix A), which means that the difference between  $\hat{H}_{st}(t)$  and  $\hat{H}_{st}(t+1)$  is smaller and therefore the influence of noise on the system evolution will be small. So a longer correlation time induces a longer valid time of the master equation.

#### IV. NUMERICAL SIMULATIONS OF NOISY DYNAMICS

Since the master equation can describe the noisy dynamics well within a certain steps  $t$ , depending on the noise parameters, to explore the long-time behavior of noisy SSQW, numerical simulations with representative noise parameters are necessary. Under the action of the Ornstein-Uhlenbeck noise, the walker spreads over the lattice with a probability distribution relevant to the amplitude  $\gamma$  and correlation time  $\tau$ . The correlation function of the Ornstein-Uhlenbeck process is similar to that of telegraph noise studied in [41]; we here choose  $\tau = 0.1$  and  $\tau = 10$ , respectively, as the typical parameters for fast noise and slow noise in this work. In Eq. (11)  $\sum_v \lambda_v(t) L_v$  can be seen as  $\hat{H}_A + \hat{H}_{A,s}$ , where  $\hat{H}_A$  is the Hamiltonian of noise and  $\hat{H}_{A,s}$  can be treated as the interaction Hamiltonian. Since this part plays the role of perturbation, one can require that the energy of this part,  $E_p$ , would be smaller than  $E_s$  (the energy of  $\hat{H}_s$ ), i.e.,  $|\langle E_p \rangle| \leq |E_s| \leq \pi$ ,  $|\langle E_p \rangle| \geq |\langle E_A \rangle| = \sqrt{3}\gamma$ . Therefore the noise amplitude  $\gamma$  should be larger than 0 but smaller than  $\sqrt{\pi^2/3}$ . In practice, in order to make the noisy dynamics more distinguishable, we consider  $\gamma \in [0, 4]$ . Moreover, we have numerically checked the dynamics for all kinds of noise parameters and found that while the probability distribution of each site may be different, the shapes of the distributions remain unchanged.

Figure 4 shows the probability distributions of the walker over lattice sites at three different evolution steps (time) with representative noise parameters. The blue lines ( $\tau = 10$  and  $\gamma = 0.1$ , a weak noise with low decaying autocorrelation function) in Figs. 4(a)–4(c) clearly show the characteristic shape of an unperturbed SSQW. Namely, two evident peaks at the edges and low probability around the initial position can be found. While two edge peaks are suppressed, the central part grows and a Gaussian-type distribution centered around the initial position arises as the noise amplitude  $\gamma$  increases [black and red lines in Figs. 4(a)–4(c)], which suggests that a transition from the quantum to classical walk occurs. The blue lines ( $\tau = 0.1$  and  $\gamma = 0.1$ , a weak noise with fast decaying autocorrelation function) in Figs. 4(d)–4(f) clearly show the destructive effect of noise on interference generated by SSQW. First, the probability distribution shows two oscillating wings at the edges and an incoherent component around the center. The central peak increases while the two oscillating wings decrease, which disappears eventually. The shapes for  $\tau = 0.1$ ,  $\gamma \geq 0.8$  are almost same [see black and red lines in Figs. 4(d)–4(f)]. From these figures we can find also that quantum effects are completely suppressed by noise in several steps, and then the oscillations are smoothed and converge towards Gaussian distributions in few lattice sites.

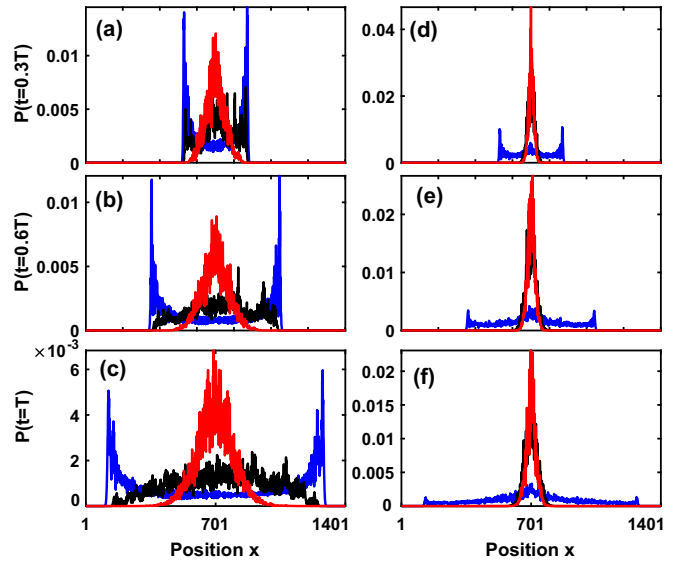


FIG. 4. Probability distribution of a walker over the lattices. The particle is initially at the localized state  $|1 + (N - 1)/2\rangle \otimes (|\uparrow\rangle - i|\downarrow\rangle)/\sqrt{2}$  with  $N = 1401$ ,  $\theta_1 = 0.2\pi$ , and  $\theta_2 = 0.3\pi$  (valid in the following work). The total number of steps is  $T = 1000$ . The noise correlation times  $\tau$  for (a)–(c) and (d)–(f) are 10 and 0.1, respectively. The blue, black, and red lines represent noise amplitudes  $\gamma = 0.1, 0.8, 4$ , respectively.

By comparing the probability distributions with the same noise amplitudes and different correlation times, one can also find that long noise correlation time is helpful to reduce the damage of noise to quantum coherence.

What emerges from our analysis so far is that in time-correlated noise regime, we see a transition from quantum ballistic transport to classical diffusion. The influence of noise on dynamics may be analyzed in more details by the time dependence of the standard deviation, as shown in Fig. 5. The first and the second moments of the spatial distribution at steps  $t$  are given by

$$\langle \overline{x(t)} \rangle = \sum_x x \langle P_t(x) \rangle \quad (21)$$

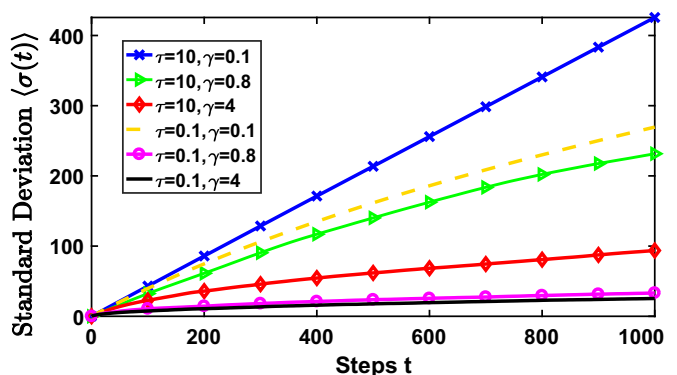


FIG. 5. The averaged standard deviation  $\langle \sigma(t) \rangle$  as a function of evolution steps for SSQW subject to noise (Ornstein-Uhlenbeck process) with different noise parameters.

and

$$\langle \overline{x^2(t)} \rangle = \sum_x x^2 \langle P_t(x) \rangle. \quad (22)$$

The standard deviation  $\langle \sigma(t) \rangle$  of noisy SSQW at time  $t$  is given by

$$\langle \sigma(t) \rangle = \sqrt{\langle \overline{x^2(t)} \rangle - \langle \overline{x(t)} \rangle^2}. \quad (23)$$

It is well known that the transport properties of DTQW are quite different from those of CRW, resulting mainly from the principle of superposition of quantum mechanics. For noiseless SSQW, the probability distribution of the walker exhibits a ballistic behavior, and  $\sigma(t) = q_0 t$ , where  $q_0 = 0.4370 \pm 0.0001$  and  $\sigma = (0.9813 \pm 0.0002)\sqrt{t}$  for CRW [48]. For  $\tau = 10$ ,  $\gamma = 0.1$ , the standard deviation is linear in time and can be expressed as  $\langle \sigma(t) \rangle = qt$  with  $q = 0.4288 \pm 0.0001$ , which is very close to the noiseless  $q_0$ . This corresponds to their high similarity of the probability distributions. And  $\langle \sigma(t) \rangle = (0.7906 \pm 0.0004)\sqrt{t}$  for  $\tau = 0.1$ ,  $\gamma = 4$  corresponding to the classical diffusion. Therefore we can conclude the standard deviations for noisy SSQW in Fig. 5 from top to bottom reflect the transition from noiseless SSQW to CRW.

So far the dynamic characteristics of the SSQW subject to time-correlated noise have been explored, and now we focus our attention on its genuine quantum features. Unitary coin operation  $R_y(\theta)$  acts only on the walker's internal degree of freedom, leaving it generally in a superposition of spin up and spin down. Conditional translation  $T_{\uparrow,\downarrow}$  relates the displacement of the walker to its internal degree of freedom. In this way, spin and position of the system are entangled, and the evolution of SSQW creates a superposition among the position states of the system, opening the way for interference effects to take place that ultimately determine the ballistic behavior for the displacement of the quantum walker. Entanglement and interference are genuine quantum features of DTQW since there are no analogs for CRW [57,58].

Consider now a many-body system divided into three regions: regions  $A$  and  $B$ , and the rest of the system,  $C$ . Assume that  $A \cup B \cup C$  is in a pure state  $|\phi\rangle$ , and let  $\rho_{AB} = \text{Tr}_C |\phi\rangle\langle\phi|$ . If  $A \cup B$  is entangled with part  $C$ , then  $\rho_{AB}$  is a mixed state. For noisy SSQW,  $A$ ,  $B$ , and  $C$  represent the coin, position, and noise, respectively.  $\text{Tr}_C$  means averaging the density matrix over possible realizations of the stochastic processes. Therefore,  $\rho(t)$  [Eq. (5)] is a mixed state, and its dynamic can be described by Eq. (17). In the following, the negativity of the averaged density matrix will be adopted to quantify the entanglement between coin and position, which is defined by [59,60]

$$N(\rho) = \frac{\|\rho^{T_x}\| - 1}{d - 1}, \quad (24)$$

where  $\|X\| = \text{Tr}\sqrt{X^\dagger X}$  denotes the trace norm of an operator  $X$ .  $\rho^{T_x}$  is the partial transpose of the state  $\rho$  in the  $d_c \otimes d_x$  ( $d_c < d_x$ ) quantum system. Here  $d_x$  and  $d_c$  represent the position degrees of freedom and coin degrees of freedom. For SSQW,  $d = 2$ , and  $\rho^{T_x}$  is defined for an orthonormal basis  $\{|x\rangle\}$  as

$$\rho^{T_x} = \sum_{x_1, x_2} (I_c \otimes |x_1\rangle\langle x_2| \rho (I_c \otimes |x_1\rangle\langle x_2|), \quad (25)$$

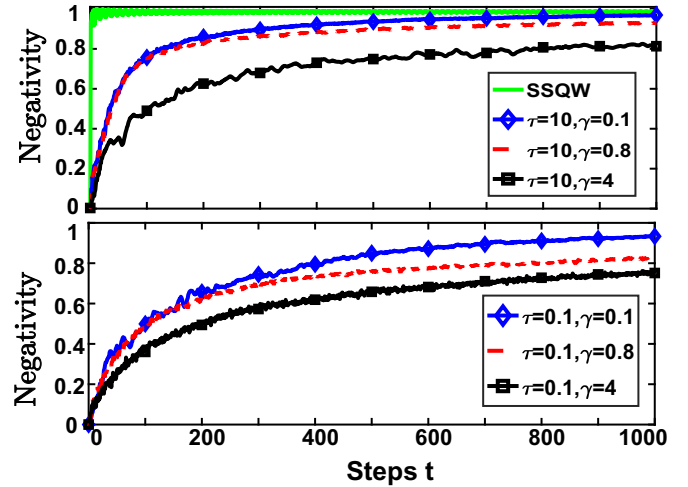


FIG. 6. Negativity as a measure of entanglement between coin and position as a function of evolution steps for SSQW subject to the Ornstein-Uhlenbeck process with different noise parameters.

where  $I_c = |\uparrow\rangle\langle\uparrow| + |\downarrow\rangle\langle\downarrow|$ . Compared with the  $N(\rho) = (\|\rho^{T_x}\| - 1)/2$ , this  $N(\rho)$  bounds the maximum value of the entanglement measure to 1 [59,60]. Besides, considering the fact that  $\log_2\{N(\rho)(d - 1) + 1\}$  reduces the Renyi entropy of a pure state  $|\phi\rangle$  with index  $q = 1/2$  [61],  $N(\rho)$  can also measure the entanglement for noiseless SSQW.

In Fig. 6 we present the negativity between the coin and position as a function of time. For noiseless SSQW, the entanglement between position and coin is realized by the protocol  $\hat{U}_s$  and approaches to the maximal value, unity, in several steps. Decreasing the noise amplitude or prolonging the correlation time, it evolves to the asymptotic values 1 more quickly. The behavior of entanglement for noisy SSQW can be understood from the role of noise in SSQW. Noise destroys the quantum features of SSQW. A transition from ballistic transport to classical Gaussian diffusion can be found in the space distribution, and the standard derivation  $\langle \sigma(t) \rangle$  changes from being proportional to steps  $t$  to being proportional to  $\sqrt{t}$ . Therefore entanglements for noisy SSQW are always smaller compared with noiseless SSQW and will cost more steps to reach its maximum.

Quantum coherence makes a QW different from the CRW, and the analysis of the probability distribution over the lattice sites and the standard derivation only involve the diagonal elements of the density matrix. In order to gain more insight into the behavior of the system, we study its coherence  $C$ . The coherence of a quantum state is investigated by adopting the normalized coherence measure proposed in [62,63]

$$\langle C(t) \rangle = \frac{1}{N - 1} \sum_{i \neq j} |\tilde{\rho}_{ij}(t)|, \quad (26)$$

where  $N$  is the dimensionality of position Hilbert space, and  $\tilde{\rho}$  is obtained by taking the trace of the averaged density matrix  $\rho(t)$  over coin degrees of freedom. Figure 7 shows the coherence for noisy SSQW with representative noise parameters. In the slow noise regime ( $\tau = 10$ ), the off-diagonal elements of the reduced density matrix grow

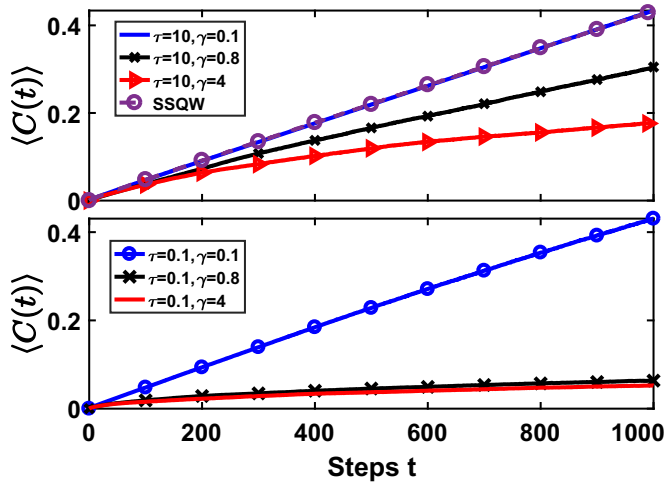


FIG. 7. Averaged coherence  $\langle C(t) \rangle$  as a function of steps  $t$  for noisy SSQW with different noise parameters.

with time, and the larger the noise amplitude  $\gamma$ , the smaller the increment of coherence during the same evolution steps. In the fast noise regime ( $\tau = 0.1$ ), the coherence  $\langle C(t) \rangle$  for  $\tau = 0.1, \gamma = 0.1$  increases over steps, but that for  $\tau = 0.1, \gamma = 0.8$  and  $\tau = 0.1, \gamma = 4$  increase quite slowly, which indicates Gaussian spatial distributions around the initial position with narrow wave packets. We also noticed that the behaviors of  $\langle C(t) \rangle$  with different noise parameters are similar to the standard derivation  $\langle \sigma(t) \rangle$  in Fig. 5. In fact, their similar behaviors are natural. Coherence describes the wave nature—the bigger the coherence, the more sites the wave packet reaches and therefore the larger the standard deviation  $\langle \sigma(t) \rangle$ .

## V. SUMMARY

We have studied the dynamics of SSQW subject to time-correlated noise, which is modeled as a coin operator before each step. The dynamics of the walker was calculated as an ensemble average over possible realizations of the noise. Based on the Hamiltonian obtained by the first-order approximation of the BCH formula, we derived the master equation of noisy SSQW, the relationship between similarity and evolution steps was calculated, and the reason was explained. In the numerical calculation part, we found that the dynamics obviously depends on the correlation time and amplitude of the stochastic process. Correlation time reflects the similarity of the stochastic process characterized by correlation function, and noise amplitude characterizes the coupling strength between the system and environment. In the fast noise regime, i.e., the similarity of a stochastic process decreases rapidly over time, noise sequence is rough; the walker undergoes time-disordered unitary evolutions and is finally confined into few lattice sites. In the slow noise regime, the spatial distribution of a weakly coupled walker clearly shows the characteristic shape of a noiseless SSQW, and a transition from quantum ballistic behavior to classical diffusive over lattice sites occurs as we increase the noise amplitude. The transition can also be observed in the standard derivation. Entanglement, as a genuine quantum feature of noisy SSQW, measured by negativity,

will approach the maximum [ $N(\rho) = 1$ ] eventually, and prolonging the correlation time or decreasing the noise amplitude can reduce the time for entanglement to reach its maximum. As for coherence, the other quantum feature, its behavior is similar to that of the standard derivation, which stresses that coherence makes QW different from CRW.

## ACKNOWLEDGMENTS

We are grateful to Jinlei Li for sharing the technical details used in the calculation. This work is supported by National Natural Science Foundation of China (NSFC) under Grant No. 11775048.

## APPENDIX A: STOCHASTIC SEQUENCE SAMPLINGS

To demonstrate the landscapes of stochastic sequences clearly, all subfigures in Fig. 8 displayed three possible noise realizations under certain noise parameters  $\tau$  and  $\gamma$ . Figure 8 illustrates two points: (1) with the same noise amplitude  $\gamma$ , the stochastic sequences with longer correlation time  $\tau$  are relatively smoother; (2) with the same noise correlation time  $\tau$ , the larger the amplitude  $\gamma$ , the more the noise deviates from the average value 0.

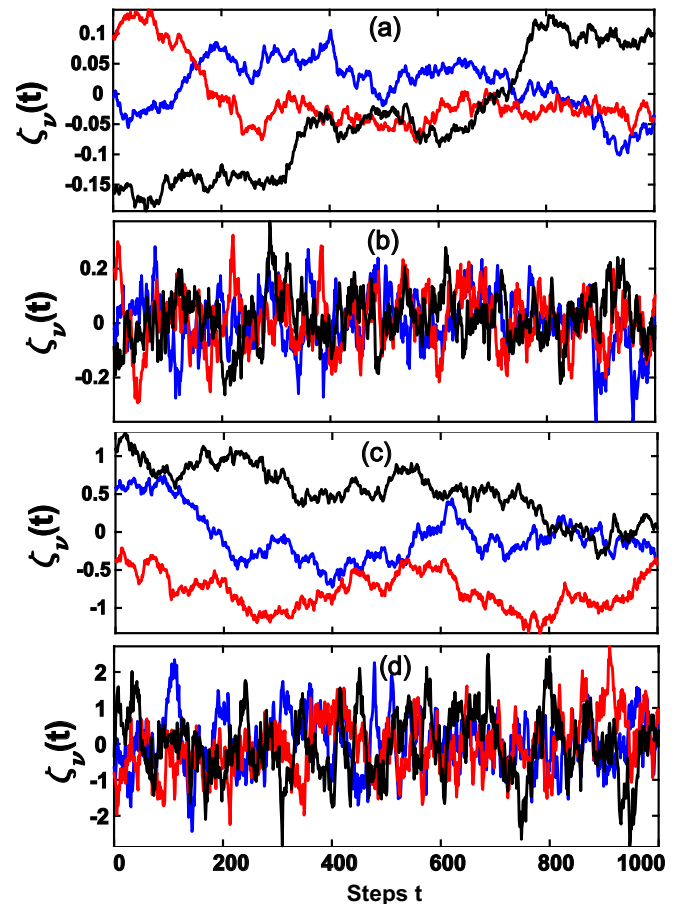


FIG. 8. The stochastic sequence landscapes:  $\tau = 10, \gamma = 0.1$ ;  $\tau = 0.1, \gamma = 0.1$ ;  $\tau = 10, \gamma = 0.8$ ; and  $\tau = 0.1, \gamma = 0.8$  for (a), (b), (c), and (d), respectively.

**APPENDIX B: DERIVATION OF THE HAMILTONIAN FOR SSQW**

Parametrized by angles  $\theta_1$  and  $\theta_2$ , a single SSQW can be defined by the time evolution operator

$$\hat{U}_s = T_\downarrow R_y(\theta_2) T_\uparrow R_y(\theta_1). \quad (\text{B1})$$

This protocol consists of two unitary rotation operations and two translation operators. Based the translational symmetry of this protocol, in the quasimomentum basis  $|k\rangle = (1/\sqrt{2\pi}) \sum_x e^{-ikx} |x\rangle$ , we can get their expressions in a quasimomentum basis as follows:

$$\begin{aligned} R_y(\theta) &= \sum_x e^{-i\theta/2\sigma_y} |x\rangle\langle x| \\ &= \sum_x e^{-i\theta/2\sigma_y} \frac{1}{\sqrt{2\pi}} \sum_{k_1} e^{ik_1x} |k_1\rangle \sum_{k_2} \frac{1}{\sqrt{2\pi}} e^{-ik_2x} \langle k_2| \\ &= \sum_{k_1, k_2} e^{-i\theta/2\sigma_y} \frac{1}{2\pi} \sum_x e^{ix(k_1-k_2)} |k_1\rangle\langle k_2| \\ &= \sum_{k_1, k_2} e^{-i\theta/2\sigma_y} \delta(k_1 - k_2) |k_1\rangle\langle k_2| \\ &= \sum_k e^{-i\theta/2\sigma_y} \otimes |k\rangle\langle k|, \\ &= \sum_k \begin{pmatrix} \cos \frac{\theta}{2} & -\sin \frac{\theta}{2} \\ \sin \frac{\theta}{2} & \cos \frac{\theta}{2} \end{pmatrix} \otimes |k\rangle\langle k|. \end{aligned} \quad (\text{B2})$$

$$\begin{aligned} T_\uparrow &= \sum_x |x+1\rangle\langle x| \otimes |\uparrow\rangle\langle\uparrow| + |x\rangle\langle x| \otimes |\downarrow\rangle\langle\downarrow| \\ &= \sum_x \sum_{k_1} \frac{1}{\sqrt{2\pi}} e^{ik_1(x+1)} |k_1\rangle \sum_{k_2} \frac{1}{\sqrt{2\pi}} e^{-ik_2x} \langle k_2| \otimes |\uparrow\rangle\langle\uparrow| + \sum_x \sum_{k_3} \frac{1}{\sqrt{2\pi}} e^{ik_3x} |k_3\rangle \sum_{k_4} \frac{1}{\sqrt{2\pi}} e^{-ik_4x} \langle k_4| \otimes |\downarrow\rangle\langle\downarrow| \\ &= \sum_{k_1, k_2} \sum_x \frac{1}{2\pi} e^{i(k_1-k_2)x} e^{ik_1} |k_1\rangle\langle k_2| \otimes |\uparrow\rangle\langle\uparrow| + \sum_{k_3, k_4} \sum_x \frac{1}{2\pi} e^{i(k_3-k_4)x} |k_3\rangle\langle k_4| \otimes |\downarrow\rangle\langle\downarrow| \\ &= \sum_{k_1, k_2} \delta(k_1 - k_2) e^{ik_1} |k_1\rangle\langle k_2| \otimes |\uparrow\rangle\langle\uparrow| + \sum_{k_3, k_4} \delta(k_3 - k_4) |k_3\rangle\langle k_4| \otimes |\downarrow\rangle\langle\downarrow| \\ &= \sum_k (e^{ik} |\uparrow\rangle\langle\uparrow| + |\downarrow\rangle\langle\downarrow|) \otimes |k\rangle\langle k| \\ &= \sum_k \begin{pmatrix} e^{ik} & 0 \\ 0 & 1 \end{pmatrix} \otimes |k\rangle\langle k|. \end{aligned} \quad (\text{B3})$$

$$\begin{aligned} T_\downarrow &= \sum_x |x\rangle\langle x| \otimes |\uparrow\rangle\langle\uparrow| + |x-1\rangle\langle x| \otimes |\downarrow\rangle\langle\downarrow| \\ &= \sum_x \sum_{k_1} \frac{1}{\sqrt{2\pi}} e^{ik_1x} |k_1\rangle \sum_{k_2} \frac{1}{\sqrt{2\pi}} e^{-ik_2x} \langle k_2| \otimes |\uparrow\rangle\langle\uparrow| + \sum_x \sum_{k_3} \frac{1}{\sqrt{2\pi}} e^{ik_3(x-1)} |k_3\rangle \sum_{k_4} \frac{1}{\sqrt{2\pi}} e^{-ik_4x} \langle k_4| \otimes |\downarrow\rangle\langle\downarrow| \\ &= \sum_{k_1, k_2} \sum_x \frac{1}{2\pi} e^{i(k_1-k_2)x} |k_1\rangle\langle k_2| \otimes |\uparrow\rangle\langle\uparrow| + \sum_{k_3, k_4} \sum_x \frac{1}{2\pi} e^{i(k_3-k_4)x} e^{-ik_3} |k_3\rangle\langle k_4| \otimes |\downarrow\rangle\langle\downarrow| \\ &= \sum_{k_1, k_2} \delta(k_1 - k_2) |k_1\rangle\langle k_2| \otimes |\uparrow\rangle\langle\uparrow| + \sum_{k_3, k_4} \delta(k_3 - k_4) e^{-ik_3} |k_3\rangle\langle k_4| \otimes |\downarrow\rangle\langle\downarrow| \\ &= \sum_k (|\uparrow\rangle\langle\uparrow| + e^{-ik} |\downarrow\rangle\langle\downarrow|) \otimes |k\rangle\langle k| \\ &= \sum_k \begin{pmatrix} 1 & 0 \\ 0 & e^{-ik} \end{pmatrix} \otimes |k\rangle\langle k|. \end{aligned} \quad (\text{B4})$$



On one hand, based on Eqs. (B2), (B3), and Eq. (B4), we can also rewrite the SSQW protocol Eq. (B1) in the quasimomentum basis as

$$\hat{U}_s = \sum_k U(k) \otimes |k\rangle\langle k|. \quad (\text{B5})$$

Therefore we can derive the expression for  $U(k)$  as follows:

$$U(k) = \begin{pmatrix} e^{ik} \cos \frac{\theta_1}{2} \cos \frac{\theta_2}{2} - \sin \frac{\theta_1}{2} \sin \frac{\theta_2}{2} & -e^{ik} \sin \frac{\theta_1}{2} \cos \frac{\theta_2}{2} - \cos \frac{\theta_1}{2} \sin \frac{\theta_2}{2} \\ e^{-ik} \sin \frac{\theta_1}{2} \cos \frac{\theta_2}{2} + \cos \frac{\theta_1}{2} \sin \frac{\theta_2}{2} & e^{-ik} \cos \frac{\theta_1}{2} \cos \frac{\theta_2}{2} - \sin \frac{\theta_1}{2} \sin \frac{\theta_2}{2} \end{pmatrix}. \quad (\text{B6})$$

Considering that  $U(k)$  is unitary, we can write

$$U(k) = e^{-iE_k \vec{n}_k \cdot \vec{\sigma}}, \quad (\text{B7})$$

where  $\vec{n}_k = (n_x, n_y, n_z)$  is the unit vector. In addition, we can always expand  $e^{-iE_k \vec{n}_k \cdot \vec{\sigma}}$  as follows:

$$e^{-iE_k \vec{n}_k \cdot \vec{\sigma}} = \begin{pmatrix} \cos E_k - i n_z \sin E_k & (-i n_x - n_y) \sin E_k \\ (-i n_x + n_y) \sin E_k & \cos E_k + i n_z \sin E_k \end{pmatrix}. \quad (\text{B8})$$

Comparing Eqs. (B4) and (B8),  $E(k)$  and  $\vec{n}(k)$  can be expressed as

$$\cos E_k = \cos(\theta_1/2) \cos(\theta_2/2) \cos k - \sin(\theta_1/2) \sin(\theta_2/2), \quad (\text{B9})$$

and

$$n_x = \frac{\sin(\theta_1/2) \cos(\theta_2/2) \sin k}{\sin E(k)}, \quad n_y = \frac{\cos(\theta_1/2) \sin(\theta_2/2) + \sin(\theta_1/2) \cos(\theta_2/2) \cos k}{\sin E(k)}, \quad n_z = \frac{-\cos(\theta_1/2) \cos(\theta_2/2) \sin k}{\sin E(k)}. \quad (\text{B10})$$

Equations (B9) and (B10) are Eqs. (9) and (10) in the main text, respectively.

On the other hand,  $\hat{U}_S$  is a unitary evolution operator, therefore

$$\hat{U}_S = e^{-i\hat{H}_S \delta t} = \sum_k e^{-iE_k \vec{n}_k \cdot \vec{\sigma}} \otimes |k\rangle\langle k|. \quad (\text{B11})$$

For QW,  $\delta t = 1$ , which means each step of evolution takes unit time. Therefore, the logarithmic result of Eq (B11) is

$$\hat{H}_S = \sum_k E_k \vec{n}_k \cdot \vec{\sigma} \otimes |k\rangle\langle k|, \quad (\text{B12})$$

which is Eq. (8) in the main text, and these derivations have been added as an Appendix.

### APPENDIX C: DERIVATION OF THE HAMILTONIAN FOR NOISY SSQW

In physics and mathematics it is often useful to write the product  $e^X e^Y$  as  $e^Z$  for some  $Z$ . When the operators  $X$  and  $Y$  do not commute, as is often the case of dealing with matrices, it may not be easy to find such a  $Z$ . Many authors attempted to deal with this problem by targeting  $Z(X, Y) = \log(e^X e^Y)$ . One of the attempts is the Baker-Campbell-Hausdorff formula

$$Z(X, Y) = X + Y + \frac{1}{2}[X, Y] + \frac{1}{12}([X, [X, Y]] + [Y, [Y, X]]) + \dots. \quad (\text{C1})$$

In our topic,  $\hat{U} = \hat{U}_s \hat{U}_A$  [Eq. (3) in the main text], where  $\hat{U}_s = e^{-i\hat{H}_s}$  and  $\hat{U}_A = e^{-i\hat{H}_A(t)}$ . Therefore  $X = -i\hat{H}_s$  and  $Y = -i\hat{H}_A(t)$ :

$$\hat{Z} = -i\hat{H}_s - i\hat{H}_A + \frac{1}{2}[-i\hat{H}_s, -i\hat{H}_A] + \frac{1}{12}([-i\hat{H}_s, [-i\hat{H}_s, -i\hat{H}_A]] + [-i\hat{H}_A, [-i\hat{H}_s, -i\hat{H}_A]]) + \dots. \quad (\text{C2})$$

In Eq. (C2), the second-order and higher-order commutators contain nonlinear terms of noise amplitude  $\lambda_\nu$ . So, up to the first-order commutator in the Baker-Campbell-Hausdorff (BCH) formula, we have

$$\hat{Z} = -i\hat{H}_s - i\hat{H}_A + \frac{1}{2}[-i\hat{H}_s, -i\hat{H}_A] = -i\hat{H}_{st}. \quad (\text{C3})$$

By the same procedure to derive Eq. (B2), we can also derive the expression of  $\hat{U}_A$  in the quasimomentum basis as follows:

$$\hat{U}_A = \sum_x e^{-i\hat{A}(t)} \otimes |x\rangle\langle x| = \sum_k e^{-i\hat{A}(t)} \otimes |k\rangle\langle k| = e^{-i\hat{H}_A}. \quad (\text{C4})$$

So, the stochastic Hamiltonian  $\hat{H}_A$  is

$$\hat{H}_A = \sum_k [\lambda_x(t) \sigma_x + \lambda_y(t) \sigma_y + \lambda_z(t) \sigma_z] \otimes |k\rangle\langle k|. \quad (\text{C5})$$

The commutation in Eq. (C3) is

$$[-i\hat{H}_S, -i\hat{H}_A] = \sum_k \hat{h}_k \otimes |k\rangle\langle k|. \quad (\text{C6})$$

The result of commutation of each  $k$  in Eq. (C6) is

$$\begin{aligned} \hat{h}_k &= -E_k[n_x\sigma_x, \lambda_x\sigma_x + \lambda_y\sigma_y + \lambda_z\sigma_z] - E_k[n_y\sigma_y, \lambda_x\sigma_x + \lambda_y\sigma_y + \lambda_z\sigma_z] - E_k[n_z\sigma_z, \lambda_x\sigma_x + \lambda_y\sigma_y + \lambda_z\sigma_z] \\ &= -E_k(n_x\lambda_y2i\sigma_z - n_x\lambda_z2i\sigma_y) - E_k(-n_y\lambda_x2i\sigma_z + n_y\lambda_z2i\sigma_x) - E_k(n_z\lambda_x2i\sigma_y - n_z\lambda_y2i\sigma_x) \\ &= 2iE_k\lambda_x(n_y\sigma_z - n_z\sigma_y) + 2iE_k\lambda_y(n_z\sigma_x - n_x\sigma_z) + 2iE_k\lambda_z(n_x\sigma_y - n_y\sigma_x) \\ &= 2i\lambda_x E_k(\vec{n} \times \vec{\sigma})_x + 2i\lambda_y E_k(\vec{n} \times \vec{\sigma})_y + 2i\lambda_z E_k(\vec{n} \times \vec{\sigma})_z. \end{aligned} \quad (\text{C7})$$

Then,  $-i\hat{H}_A + \frac{1}{2}[-i\hat{H}_S, -i\hat{H}_A] = \sum_k \hat{h}_{SA} \otimes |k\rangle\langle k|$ ,

$$\begin{aligned} \hat{h}_{SA} &= -i[\lambda_x(t)\sigma_x + \lambda_y(t)\sigma_y + \lambda_z(t)\sigma_z] + i\lambda_x E_k(\vec{n} \times \vec{\sigma})_x + i\lambda_y E_k(\vec{n} \times \vec{\sigma})_y + i\lambda_z E_k(\vec{n} \times \vec{\sigma})_z \\ &= -i\lambda_x(t)[\sigma_x - E_k(\vec{n} \times \vec{\sigma})_x] - i\lambda_y(t)[\sigma_y - E_k(\vec{n} \times \vec{\sigma})_y] - i\lambda_z(t)[\sigma_z - E_k(\vec{n} \times \vec{\sigma})_z] \\ &= -i[\lambda_x(t)\hat{L}_x + \lambda_y(t)\hat{L}_y + \lambda_z(t)\hat{L}_z]. \end{aligned} \quad (\text{C8})$$

Therefore

$$\hat{L}_x = \sum_k [\sigma_x - E_k(\vec{n} \times \vec{\sigma})_x] \otimes |k\rangle\langle k|, \quad \hat{L}_y = \sum_k [\sigma_y - E_k(\vec{n} \times \vec{\sigma})_y] \otimes |k\rangle\langle k|, \quad \hat{L}_z = \sum_k [\sigma_z - E_k(\vec{n} \times \vec{\sigma})_z] \otimes |k\rangle\langle k|. \quad (\text{C9})$$

Equation (C9) is Eq. (12) in the main text.

- 
- [1] Y. Aharonov, L. Davidovich, and N. Zagury, Quantum random walks, *Phys. Rev. A* **48**, 1687 (1993).
- [2] E. Farhi and S. Gutmann, Quantum computation and decision trees, *Phys. Rev. A* **58**, 915 (1998).
- [3] J. Kempe, Quantum random walks: An introductory overview, *Comtemp. Phys.* **44**, 307 (2003).
- [4] A. M. Childs and J. Goldstone, Spatial search by quantum walk, *Phys. Rev. A* **70**, 022314 (2004).
- [5] A. M. Childs, Universal Computation by Quantum Walk, *Phys. Rev. Lett.* **102**, 180501 (2009).
- [6] R. J. Sension, Quantum path to photosynthesis, *Nature (London)* **446**, 740 (2007).
- [7] G. S. Engel, T. R. Calhoun, E. L. Read, T. K. Ahn, T. Manal, Y. C. Cheng, R. E. Blankenship, and G. R. Fleming, Evidence for wavelike energy transfer through quantum coherence in photosynthetic systems, *Nature (London)* **446**, 782 (2007).
- [8] M. Mohseni, P. Rebentrost, S. Lloyd, and A. Aspuru-Guzik, Environment assisted quantum walks in photosynthetic energy transfer, *J. Chem. Phys.* **129**, 174106 (2008).
- [9] S. Godoy and S. Fujita, A quantum random walk model for tunneling diffusion in a 1D lattice. A quantum correction to Fick's law, *J. Chem. Phys.* **97**, 5148 (1992).
- [10] M. S. Rudner and L. S. Levitov, Topological Transition in a Non-Hermitian Quantum Walk, *Phys. Rev. Lett.* **102**, 065703 (2009).
- [11] S. Hoyer and D. A. Meyer, Faster transport with a directed quantum walk, *Phys. Rev. A* **79**, 024307 (2009).
- [12] T. Oka, N. Konno, R. Arita, and H. Aoki, Breakdown of an Electric-Field Driven System: A Mapping to a Quantum Walk, *Phys. Rev. Lett.* **94**, 100602 (2005).
- [13] C. Lyu, Luyan Yu, and S. Wu, Localization in quantum walks on a honeycomb network, *Phys. Rev. A* **92**, 052305 (2015).
- [14] X. P. Xu, Y. Ide, and N. Konno, Symmetry and localization of quantum walks induced by an extra link in cycles, *Phys. Rev. A* **85**, 042327 (2012).
- [15] J. K. Asbóth and H. Obuse, Bulk-boundary correspondence for chiral symmetric quantum walks, *Phys. Rev. B* **88**, 121406(R) (2013).
- [16] E. Flurin, V. V. Ramasesh, S. Hacoheh-Gourgy, L. S. Martin, N. Y. Yao, and I. Siddiqi, Observing Topological Invariants Using Quantum Walks in Superconducting Circuits, *Phys. Rev. X* **7**, 031023 (2017).
- [17] X. P. Wang, L. Xiao, X. Z. Qiu, K. k. Wang, W. Yi, and P. Xue, Detecting topological invariants and revealing topological phase transitions in discrete-time photonic quantum walks, *Phys. Rev. A* **98**, 013835 (2018).
- [18] X. Zhan, L. Xiao, Z. Bian, K. Wang, X. Qiu, B. C. Sanders, W. Yi, and P. Xue, Detecting Topological Invariants in Nonunitary Discrete-Time Quantum Walks, *Phys. Rev. Lett.* **119**, 130501 (2017).
- [19] L. Xiao, X. Z. Qiu, K. k. Wang, Z. H. Bian, X. Zhan, H. Obuse, B. C. Sanders, W. Yi, and P. Xue, Higher winding number in a nonunitary photonic quantum walk, *Phys. Rev. A* **98**, 063847 (2018).
- [20] T. Kitagawa, M. S. Rudner, E. Berg, and E. Demler, Exploring topological phases with quantum walks, *Phys. Rev. A* **82**, 033429 (2010).
- [21] W. Dür, R. Raussendorf, V. M. Kendon, and H. J. Briegel, Quantum walks in optical lattices, *Phys. Rev. A* **66**, 052319 (2002).
- [22] L. M. Wang, L. Wang, and Y. B. Zhang, Quantum walks of two interacting anyons in one dimensional optical lattices, *Phys. Rev. A* **90**, 063618 (2014).
- [23] H. Schmitz, R. Matjeschk, Ch. Schneider, J. Glueckert, M. Enderlein, T. Huber, and T. Schaetz, Quantum Walk of a

- Trapped Ion in Phase Space, *Phys. Rev. Lett.* **103**, 090504 (2009).
- [24] F. Zähringer, G. Kirchmair, R. Gerritsma, E. Solano, R. Blatt, and C. F. Roos, Realization of a Quantum Walk with One and Two Trapped Ions, *Phys. Rev. Lett.* **104**, 100503 (2010).
- [25] A. R. C. Buarque and W. S. Dias, Self-trapped quantum walks, *Phys. Rev. A* **101**, 023802 (2020).
- [26] A. Schreiber, K. N. Cassemiro, V. Potoček, A. Gabris, P. J. Mosley, E. Andersson, I. Jex, and Ch. Silberhorn, Photons Walking the Line: A Quantum Walk with Adjustable Coin Operations, *Phys. Rev. Lett.* **104**, 050502 (2010).
- [27] A. Schreiber, A. Gábris, P. P. Rohde, K. Laiho, M. Štefaňák, V. Potoček, C. Hamilton, I. Jex, and C. Silberhorn, A 2D quantum walk simulation of two-particle dynamics, *Science* **336**, 55 (2012).
- [28] A. W. Eddins, C. C. Beedle, D. N. Hendrickson, and J. R. Friedman, Collective Coupling of a Macroscopic Number of Single-Molecule Magnets with a Microwave Cavity Mode, *Phys. Rev. Lett.* **112**, 120501 (2014).
- [29] B. Wang, T. Chen, and X. Zhang, Experimental Observation of Topologically Protected Bound States with Vanishing Chern Numbers in a Two-Dimensional Quantum Walk, *Phys. Rev. Lett.* **121**, 100501 (2018).
- [30] C. Chen, X. Ding, J. Qin, Y. He, Y. Luo, M. Chen, C. Liu, X. Wang, W. Zhang, H. Li, L. You, Z. Wang, D. Wang, B. C. Sanders, C. Y. Lu, and J. W. Pan, Observation of Topologically Protected Edge States in a Photonic Two-Dimensional Quantum Walk, *Phys. Rev. Lett.* **121**, 100502 (2018).
- [31] M. A. Broome, A. Fedrizzi, B. P. Lanyon, I. Kassal, A. Aspuru-Guzik, and A. G. White, Discrete Single-Photon Quantum Walks with Tunable Decoherence, *Phys. Rev. Lett.* **104**, 153602 (2010).
- [32] C. A. Ryan, M. Laforest, J. C. Boileau, and R. Laflamme, Experimental implementation of a discrete-time quantum random walk on an NMR quantum-information processor, *Phys. Rev. A* **72**, 062317 (2005).
- [33] J. Du, H. Li, X. Xu, M. Shi, J. Wu, X. Zhou, and R. Han, Experimental implementation of the quantum random-walk algorithm, *Phys. Rev. A* **67**, 042316 (2003).
- [34] L. Wang, N. Liu, S. Chen, and Y. Zhang, Quantum walks accompanied by spin flipping in one-dimensional optical lattices, *Phys. Rev. A* **92**, 053606 (2015).
- [35] S. E. V. Andraca, Quantum walks: a comprehensive review, *Quantum Inf. Process.* **11**, 1501 (2012).
- [36] P. L. Knight, E. Roldán, and J. E. Sipe, Quantum walk on the line as an interference phenomenon, *Phys. Rev. A* **68**, 020301(R) (2003).
- [37] C. M. Chandrashekar, Disordered-quantum-walk-induced localization of a Bose-Einstein condensate, *Phys. Rev. A* **83**, 022320 (2011).
- [38] H. Jeong, M. Paternostro, and M. S. Kim, Simulation of quantum random walks using the interference of a classical field, *Phys. Rev. A* **69**, 012310 (2004).
- [39] V. Kendon and B. C. Sanders, Complementarity and quantum walks, *Phys. Rev. A* **71**, 022307 (2005).
- [40] E. Abrahams, P. W. Anderson, D. C. Licciardello, and T. V. Ramakrishnan, Scaling Theory of Localization: Absence of Quantum Diffusion in Two Dimensions, *Phys. Rev. Lett.* **42**, 673 (1979).
- [41] C. Benedetti, F. Buscemi, P. Bordone, and M. G. A. Paris, Non-Markovian continuous-time quantum walks on lattices with dynamical noise, *Phys. Rev. A* **93**, 042313 (2016).
- [42] K. Byczuk, W. Hofstetter, and D. Vollhardt, Mott-Hubbard Transition versus Anderson Localization in Correlated Electron Systems with Disorder, *Phys. Rev. Lett.* **94**, 056404 (2005).
- [43] I. Siloi, C. Benedetti, E. Piccinini, J. Piilo, S. Maniscalco, M. G. A. Paris, and P. Bordone, Noisy quantum walks of two indistinguishable interacting particles, *Phys. Rev. A* **95**, 022106 (2017).
- [44] S. E. V. Andraca, J. L. Ball, K. Burnett, and S. Bose, Quantum walks with entangled coins, *New J. Phys.* **7**, 221 (2005).
- [45] N. Inui and N. Konno, Localization of multi-state quantum walk in one dimension, *Physica A* **353**, 133 (2005).
- [46] N. Inui, N. Konno, and E. Segawa, One-dimensional three-state quantum walk, *Phys. Rev. E* **72**, 056112 (2005).
- [47] P. Ribeiro, P. Milman, and R. Mosseri, Aperiodic Quantum Random Walks, *Phys. Rev. Lett.* **93**, 190503 (2004).
- [48] D. Shapira, O. Biham, A. J. Bracken, and M. Hackett, One-dimensional quantum walk with unitary noise, *Phys. Rev. A* **68**, 062315 (2003).
- [49] A. Schreiber, K. N. Cassemiro, V. Potoček, A. Gábris, I. Jex, and Ch. Silberhorn, Decoherence and Disorder in Quantum Walks: From Ballistic Spread to Localization, *Phys. Rev. Lett.* **106**, 180403 (2011).
- [50] J. M. Edge and J. K. Asboth, Localization, delocalization, and topological transitions in disordered two-dimensional quantum walks, *Phys. Rev. B* **91**, 104202 (2015).
- [51] D. Shapira, S. Mozes, and O. Biham, Effect of unitary noise on Grover's quantum search algorithm, *Phys. Rev. A* **67**, 042301 (2003).
- [52] D. Hocker, C. Brif, M. D. Grace, A. Donovan, T.-S. Ho, K. M. Tibbetts, R. Wu, and H. Rabitz, Characterization of control noise effects in optimal quantum unitary dynamics, *Phys. Rev. A* **90**, 062309 (2014).
- [53] A. Chenu, M. Beau, J. Cao, and A. del Campo, Quantum Simulation of Generic Many-Body Open System Dynamics Using Classical Noise, *Phys. Rev. Lett.* **118**, 140403 (2017).
- [54] M. A. C. Rossi, C. Benedetti, M. Borrelli, S. Maniscalco, and M. G. A. Paris, Continuous-time quantum walks on spatially correlated noisy lattices, *Phys. Rev. A* **96**, 040301(R) (2017).
- [55] C. V. C. Mendes, G. M. A. Almeida, M. L. Lyra, and F. A. B. F. de Moura, Localization-delocalization transition in discrete-time quantum walks with long-range correlated disorder, *Phys. Rev. E* **99**, 022117 (2019).
- [56] E. A. Novikov, Functions and the random-force method in turbulence theory, *JETP* **20**, 1290 (1965).
- [57] T. Chen, X. Zhang, and X. D. Zhang, Quantum sensing of noises in one and two dimensional quantum walks, *Sci. Rep.* **7**, 4962 (2017).
- [58] R. Vieira, E. P. M. Amorim, and G. Rigolin, Entangling power of disordered quantum walks, *Phys. Rev. A* **89**, 042307 (2014).
- [59] T. Machida and C. M. Chandrashekar, Localization and limit laws of a three-state alternate quantum walk on a two-dimensional lattice, *Phys. Rev. A* **92**, 062307 (2015).

- [60] J. Wesenberg and K. Mølmer, Mixed collective states of many spins, *Phys. Rev. A* **65**, 062304 (2002).
- [61] Y. A. Lee and G. Vidal, Entanglement negativity and topological order, *Phys. Rev. A* **88**, 042318 (2013).
- [62] T. Baumgratz, M. Cramer, and M. B. Plenio, Quantifying Coherence, *Phys. Rev. Lett.* **113**, 140401 (2014).
- [63] M. N. Bera, T. Qureshi, M. A. Siddiqui, and A. K. Pati, Duality of quantum coherence and path distinguish ability, *Phys. Rev. A* **92**, 012118 (2015).